JOURNAL OF MATERIALS SCIENCE 17 (1982) 1017–1035

Plastic deformation and solid-phase transformation in polybutene-1

E. WEYNANT, J. M. HAUDIN
Centre de Mise en Forme des Matériaux, Ecole des Mines de Paris, ERA au CNRS no. 837, Sophia Antipolis, 06560 Valbonne, France

C. G'SELL
Laboratoire de Physique du Solide, Ecole des Mines de Nancy, LA au CNRS no. 155, Parc de Saurupt, 54042 Nancy, France

The stress–strain behaviour under uniaxial tension was investigated for polybutene-1 specimens crystallized in Modification II with various types of spherulitic microstructure and degrees of crystallinity. As for Modification I, the tensile properties were found to depend greatly on the initial microstructure, but Modification II specimens exhibit a much more pronounced plastic behaviour than specimens fully transformed into Modification I prior to deformation. The deformation of spherulites within the samples was followed either by direct microscopic observation or by means of small-angle light scattering patterns. *In situ* microscopic observations of individual spherulites showed that the characteristic dark band, which appeared in the early stages of the deformation of Modification I spherulites and which corresponds to the whitening of the strained samples when observed with reflected light, occurred for much larger strains in the case of specimens initially crystallized in Modification II. Differential scanning calorimetry and wide-angle X-ray scattering experiments performed before and after the tensile tests ensured that the unstable tetragonal Modification II was transformed into the stable hexagonal Modification I during the plastic deformation. Eventually, the evolution of this phase transformation was determined as a function of the applied tensile strain by use of X-ray diffractometry.

1. Introduction

With respect to other polyolefins, isotactic polybutene-1 exhibits an original polymorphism. Several polymorphic forms have been described in the literature: rhombohedral (or hexagonal) Modification I [1] and I′ [2, 3], tetragonal Modification II [4, 5] and orthorhombic Modification III [6, 7]. Among them, the most important ones are Modifications I and II. The tetragonal Modification II is obtained by crystallization from the melt at pressures below 1000 atm. It is unstable and undergoes a spontaneous, irreversible crystal–crystal transformation into the stable, hexagonal Modification I [8–12]. This transformation involves a change in the chain conformation: the 11_3 helix of Modification II converts into a 3_1 helix in Modification I. Such a structural change requires an elongation of the helical axis.

The II → I transformation rate is affected by various chemical or mechanical factors, such as molecular weight and tacticity [13], co-polymerization [14], nucleating agents [12, 15], hydrostatic pressure [1, 3, 8, 12], mechanical deformation [1, 3, 4, 8, 12, 16, 17], orientation [9], etc. Many authors have pointed out that the transformation can be greatly accelerated by stretching [1, 3, 4, 8, 12, 17], but there is, in comparison, little previous work describing the structural and morphological changes which occur during the deformation. For instance, the defor-

0022–2461/82/041017–19$04.78/0

mation of spherulitic specimens, initially crystallized in Modification II, has been investigated by Yang and Stein [16] by means of microscopic observations and bi-refringence measurements.

The present work is concerned with the deformation and rupture of polybutene-1 specimens, initially crystallized in Modification II with different types of spherulitic microstructures. As in a previous paper [18] devoted to the deformation of Modification I spherulites, particular attention was paid to the correlation between spherulite morphology and macroscopic mechanical behaviour. In the same way, the deformation of individual spherulites was characterized during uniaxial tensile tests by *in situ* observations. Lastly, the evolution of the II to I transformation was reported at different stages of the deformation.

2. Experimental details

2.1. Sample preparation

The polybutene-1 used in this study was an experimental grade supplied by courtesy of CdF Chimie (grade 0.5, molecular weight, M_W = 550000, density 0.910). Films were prepared by pressing the molten polymer at 170° C between two glass slides and then crystallizing it. As shown in the previous work [18], a wide range of spherulite morphologies can be obtained with suitable crystallization temperatures. All the tensile tests reported in this paper were performed immediately after the crystallization process. In such conditions specimens only contained the unstable Modification II.

2.2. Tensile tests

The stress–strain behaviour of the material was determined at room temperature with an Instron tensile testing machine. Samples were carefully cut out of the films, in order to prevent the II → I transformation. For *in situ* observation of the spherulite deformation and for X-ray experiments during the course of a tensile test, we used a special miniaturized tensile machine, the principle of which has been described previously [18].

2.3. Other techniques

The melting point and the degree of crystallinity of the samples were determined by differential scanning calorimetry (Perkin Elmer DSC 2 calorimeter). The evolution of microstructures with small spherulites was followed by the small-angle light scattering technique (SALS). Finally, the transformation II → I was characterized by wide-angle X-ray scattering, either by the flat-film camera technique (filtered CuKα radiation) or by diffractometry (monochromatic CuKα_1 radiation). X-ray diffraction also provided information on the crystalline orientation in strained specimens.

3. Results

As in the previous paper [18], specimens with five types of microstructure were obtained by crystallization from the melt with five different techniques:

Type 1: Crystallization during quenching in liquid nitrogen.

Type 2: Crystallization during quenching in iced water.

Type 3: Crystallization in air at 25° C.

Type 4: Crystallization in air at 75° C.

Type 5: Crystallization during a controlled cooling at 0.2° C min^{-1} in a regulated hot stage (spherulites appeared at 102° C and crystallization was completed at 80° C).

Just after the crystallization process all the specimens were crystallized in the unstable Modification II. For the five types of microstructure, the spherulite diameters were determined either by direct microscopic observation or by small-angle light scattering [19]. Table I shows that the various crystallization procedures led to spherulite diameters ranging from 1 μm (specimens quenched in liquid nitrogen) to more than 1 mm (slowly cooled specimens). These values are the same as for Modification I [18]. Furthermore, the SALS patterns are similar to those obtained after complete transformation into Modification I [18]. So, as already indicated by several authors [20, 21], it can be concluded that the II → I transformation affects neither the spherulite size, nor the arrangement of crystallites within the spherulites.

In addition to this geometrical characterization of the spherulites, a complementary study was performed by differential scanning calorimetry in order to determine for each type of microstructure the melting temperature, the enthalpy of fusion and the degree of crystallinity. The results, also reported in Table I, show that the weight fraction of polymer crystallized in Modification II increases from 36.6% in Type 1 to 51.1% in Type 5. These degrees of crystallinity are lower than the ones of specimens crystallized in Modification I with the same crystallization procedures [18].

TABLE I Main structural features of the five types of microstructure

Type of microstructure	Spherulitic diameter (μm)	Melting temperature T_m (° C)	Enthalpy of fusion per unit mass ΔH_m (cal g^{-1})	Weight fraction crystallinity (%)
1	1	106	6.6	36.6
2	15	108	6.7	37.5
3	60	108	7.6	42.2
4	400	109	8.7	48.6
5	1100	110	9.2	51.1

3.1. Tensile testing of polybutene samples in Modification II

Specimens crystallized in Modification II with the five types of microstructure described above were tested in tension at constant elongation rate on an Instron tensile testing machine, in order to derive their stress–strain behaviour. The nominal strain rate was equal to 6×10^{-3} sec^{-1}. Fig. 1 shows the nominal stress–strain curves, obtained directly from the load–elongation charts. None of the samples exhibits any yield drop, which can be related to the observation of a fully homogeneous deformation (no necking process). Thanks to this property, the true stress against true strain plot can be easily derived using the following equations: $\sigma = \sigma_N (1 + \epsilon_N)$; $\epsilon = ln (1 + \epsilon_N)$. This representation leads to the curves displayed in Fig. 2, which call for the following remarks:

(a) The initial mechanical behaviour (viscoelastic range) is characterized by a low initial modulus and is limited by a low yield stress of a few MPa. This value is smaller the lower the spherulite size and the degree of crystallinity.

(b) A second stage begins for a strain about 0.05. Its consolidation rate, $d\sigma/d\epsilon$, is initially very small (about 20 MPa) and it increases gradually as the deformation proceeds, up to about 100 MPa just before rupture. Unloading of the specimens (Fig. 3) during the tensile test shows that the short-term elastic recovery drops rapidly as strain increases, from about 60% to about 20%. So the strain is essentially due to the plastic deformation mechanism. Even if it was assumed that the plastic deformation of such a ductile polymer could present some features of reversibility [22–25], we showed that the characteristic time for the recovery of the plastic deformation in polybutene should be of several orders of magnitude longer than the viscoelastic recovery [26].

(c) The plastic range is terminated by the rupture of the specimen, which occurs in a brittle way in specimens with large and well-crystallized spherulites (Types 3 to 5) and in a more ductile and fibrillar way in specimens with finer microstructures (Types 1 and 2). One notes also that the strain at rupture is smaller for the former than for the latter specimens ($\epsilon_r \sim 0.55$ for specimens of Type 5 and $\epsilon_r \sim 1.6$ for specimens of Type 1).

In the course of the tensile tests, a gross optical observation showed that specimens with microstructures of Types 1 and 2 kept their initial translucence up to rupture. Conversely, specimens of Types 3 to 5 began to whiten for strains

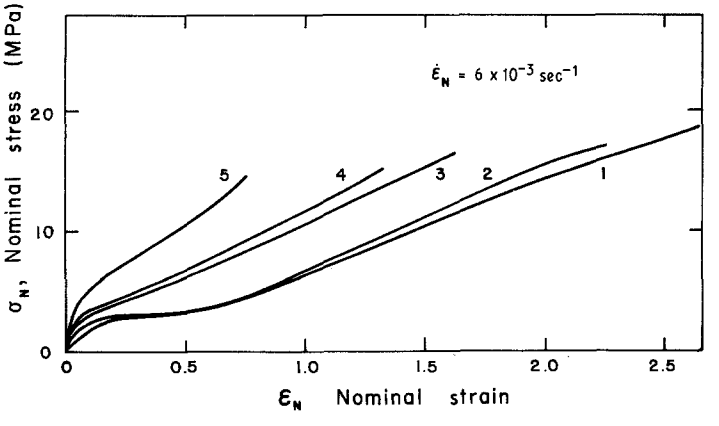

Figure 1 Nominal stress against nominal strain for the specimens crystallized in Modification II with the five different types of microstructure.

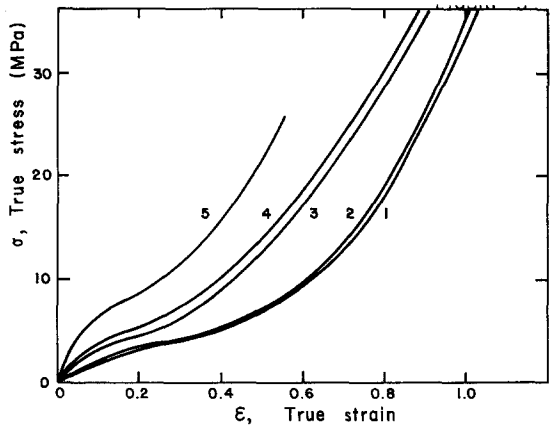

Figure 2 True stress against true strain deduced from the data of Fig. 1.

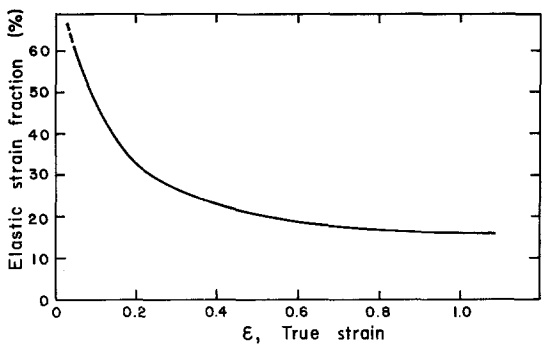

Figure 3 Evolution of the elastic strain fraction as a function of the total true strain for a specimen crystallized in air at 25° C (microstructure Type 3).

equal to about 0.29, 0.51 and 0.54, respectively. This whitening, which develops gradually and is essentially irreversible, makes the material opaque when observed with transmitted light.

It seems worthwhile at this stage of the investigation to compare the above results with those of specimens transformed into Modification I prior to deformation [18]. While Modification I exhibits all the characteristics of a hard elastic material (high degree of elastic reversibility, higher yield stress), polybutene in Modification II has a more pronounced plastic character (Fig. 4). However, one may note that its consolidation rate rapidly becomes higher, so that the ultimate tensile stress is higher than for Modification I. Concerning the microstructural evolution, it appears that the whitening occurs far later for Modification II than for Modification I specimens, in which we observed that the whitening appeared for strains as low as 0.1 [18].

3.2. *In situ* fine-scale observation of spherulite deformation

Having characterized the mechanical properties of freshly crystallized polybutene, we shall now turn our attention to the plastic response of the material at the scale of individual spherulites. For microstructures with large and well-crystallized spherulites, this characterization will be made by a direct *in situ* microscopic technique, while for microstructures with small spherulites, their evolution will be followed in an indirect way through the observation of SALS patterns.

3.2.1. Observation by optical microscopy

As shown previously [18], the observation of the deformation of large spherulites in completely crystallized specimens is limited by the early brittle rupture. So, it is more convenient to perform such observations in specially prepared samples where a few large spherulites are embedded in a soft microspherulitic matrix. Such a microstructure is easily obtained by an incomplete crystallization

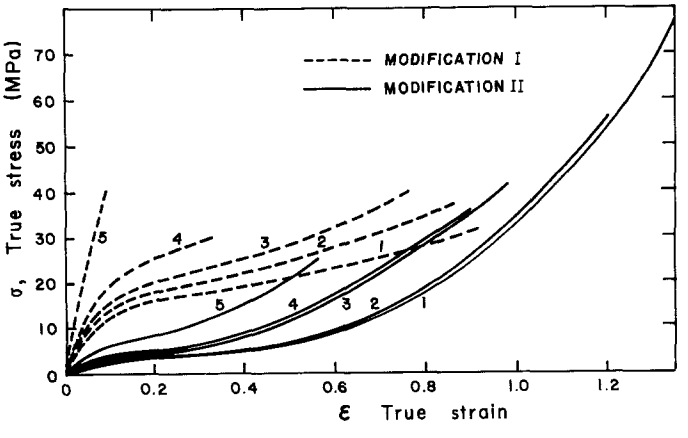

Figure 4 True stress–strain curves of Modification II samples compared with those of specimens obtained with the same crystallization procedures and transformed into Modification I prior to deformation.

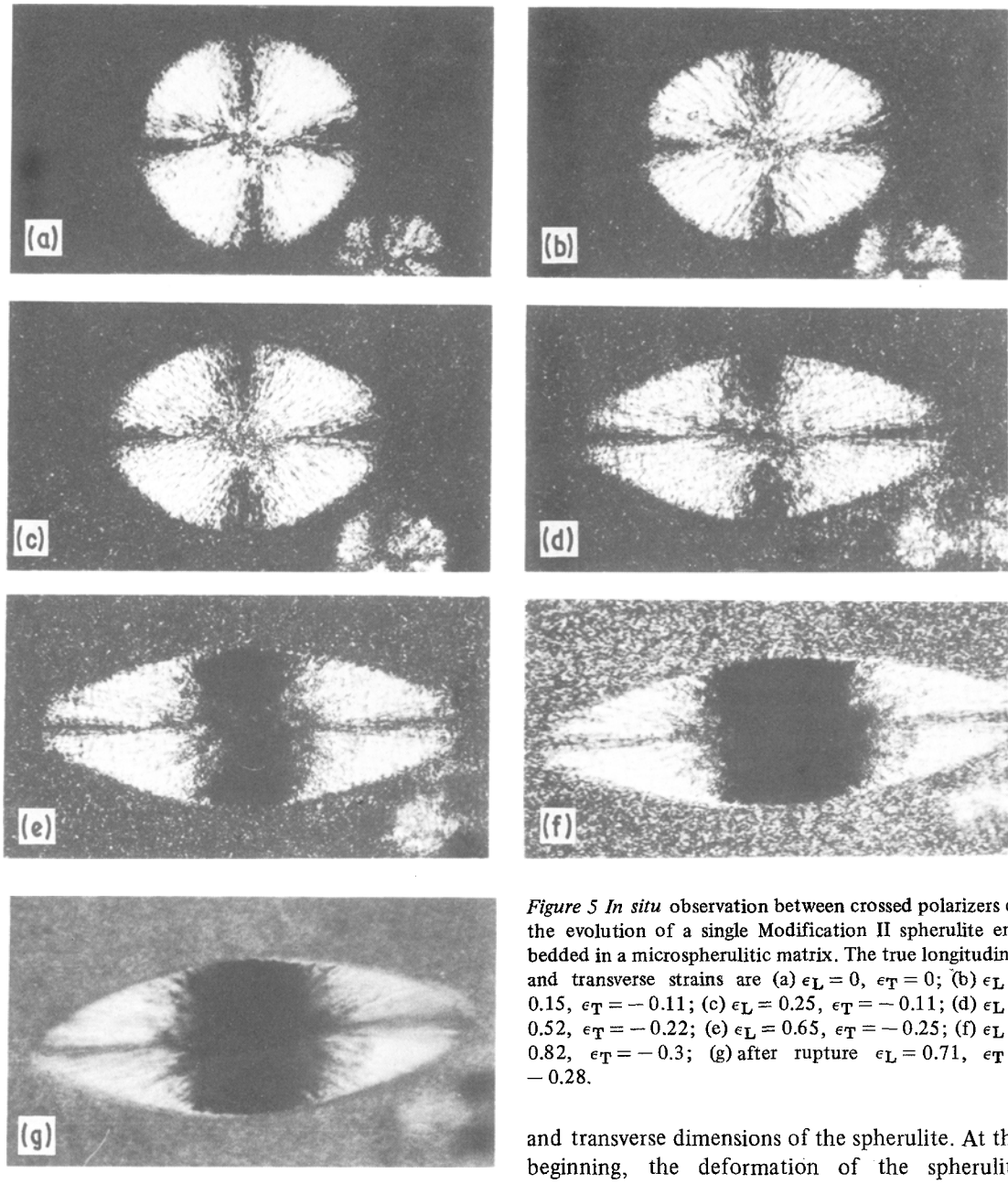

Figure 5 In situ observation between crossed polarizers of the evolution of a single Modification II spherulite embedded in a microspherulitic matrix. The true longitudinal and transverse strains are (a) $\epsilon_L = 0$, $\epsilon_T = 0$; (b) $\epsilon_L = 0.15$, $\epsilon_T = -0.11$; (c) $\epsilon_L = 0.25$, $\epsilon_T = -0.11$; (d) $\epsilon_L = 0.52$, $\epsilon_T = -0.22$; (e) $\epsilon_L = 0.65$, $\epsilon_T = -0.25$; (f) $\epsilon_L = 0.82$, $\epsilon_T = -0.3$; (g) after rupture $\epsilon_L = 0.71$, $\epsilon_T = -0.28$.

at 90° C, followed by rapid quenching in iced water.

Fig. 5 shows some stages of the evolution of a typical spherulite (diameter 200 μm) in a matrix of spherulites with diameters of about 10 μm. For each step of the deformation, a micrograph obtained with crossed polarizers is presented. The values of the local longitudinal true strain, ϵ_L, and of the transverse true strain, ϵ_T, were determined from direct measurements of the longitudinal and transverse dimensions of the spherulite. At the beginning, the deformation of the spherulite proceeds by its general elongation in the tensile direction (Fig. 5b and c) and does not present, as observed in other polymers [24, 27, 28], any major inhomogeneity, such as micronecking. Only after the longitudinal strain has reached 0.52 (Fig. 5d) is a local darkening unambiguously observed in the equatorial region of the spherulite, perpendicular to the tensile axis. It gradually turns into a broad dark band, which tends to spread over the whole surface of the spherulite (Fig. 5e and f). Micrographs 5f and g were taken, respectively, just before and after rupture, which occurred in

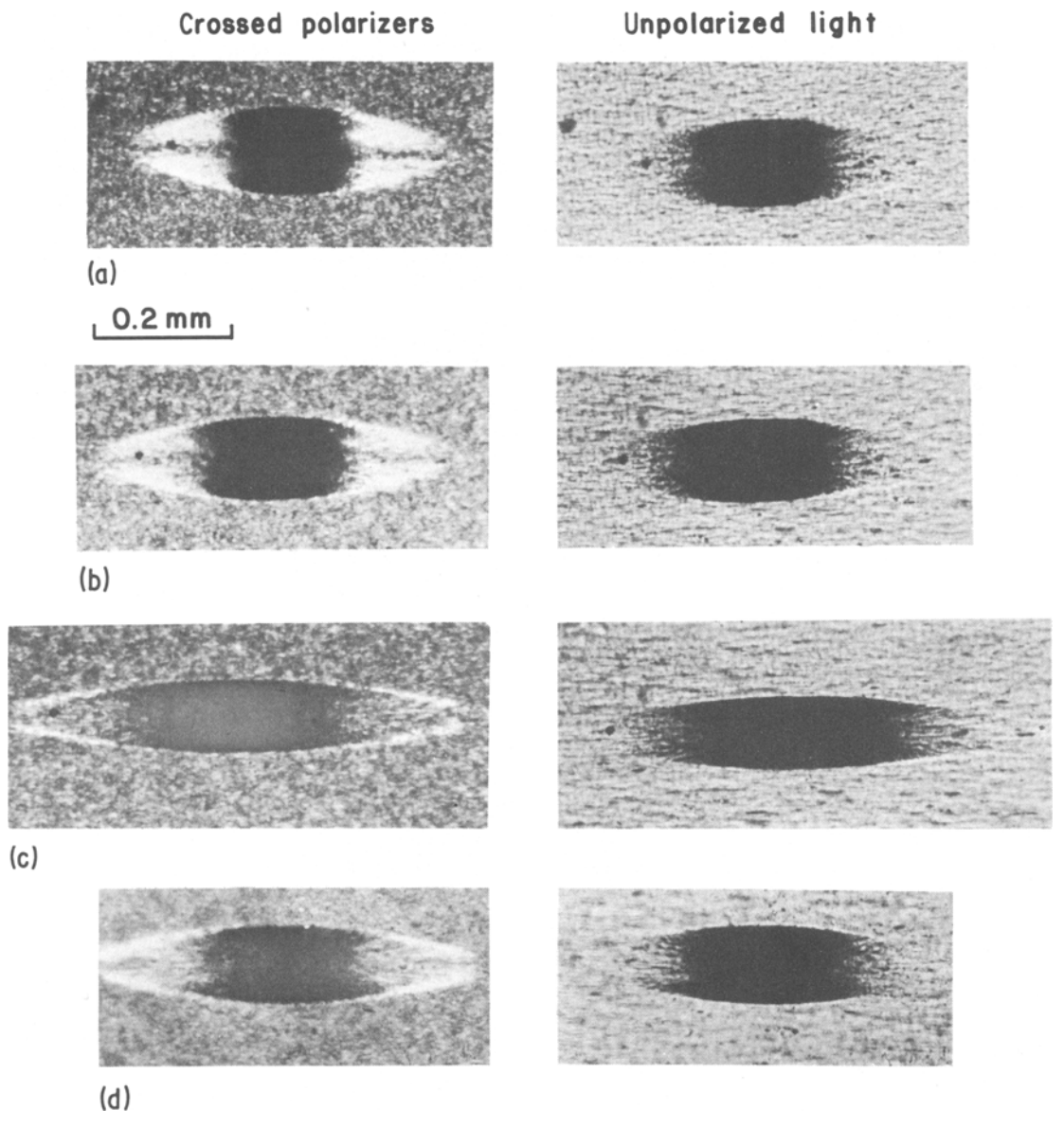

Figure 6 In situ observation under large longitudinal true strain of the evolution of an individual spherulite initially crystallized in Modification II. For each step of the deformation the spherulite is observed with crossed polarizers parallel and perpendicular to the tensile axis and unpolarized light. The true strains are: (a) $\epsilon_L = 0.86$, $\epsilon_T = -0.43$; (b) $\epsilon_L = 1.00$, $\epsilon_T = -0.49$; (c) $\epsilon_L = 1.22$, $\epsilon_T = -0.60$; (d) after rupture $\epsilon_L = 1.07$, $\epsilon_T = -0.52$.

another region of the specimen. It can be seen that the viscoelastic recovery is only 13% of the total longitudinal strain. As described above in macroscopic tensile tests, this microscopic characterization showed that the deformation of spherulites in Phase II is less reversible than in Phase I.

The evolution of the dark equatorial band for large strains was shown by a complementary study performed on another specimen (Fig. 6). For this specimen, microscopic observations were systematically performed in two different ways: between crossed polarizers and with unpolarized light. As for Modification I [18], the dark band is visible with unpolarized light as well as with crossed polarizers. It can be seen that for large strains, the dark region extends over almost the whole surface of the spherulite. After rupture, the viscoelastic recovery represents 12% of the total longitudinal strain.

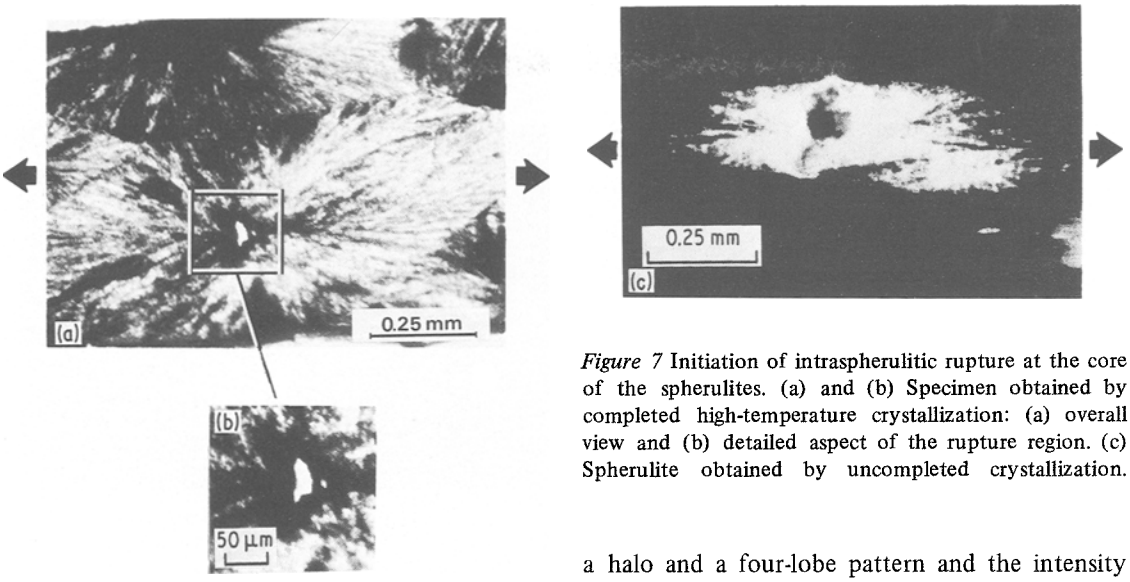

Figure 7 Initiation of intraspherulitic rupture at the core of the spherulites. (a) and (b) Specimen obtained by completed high-temperature crystallization: (a) overall view and (b) detailed aspect of the rupture region. (c) Spherulite obtained by uncompleted crystallization.

For Fig. 5 as well as for Fig. 6, the evolution of the fine spherulites in the microspherulitic matrix could not be followed at the chosen magnification by optical microscopy. Nevertheless, it was observed that with increasing strain the matrix became gradually coloured according to the different interference colours, which is indicative of an orientation of the chains towards the stretching direction.

As for Modification I specimens, many microscopic observations proved that rupture occurs in specimens initially crystallized in Modification II by an intraspherulitic process. The micrographs of Fig. 7 obtained by completed (Fig. 7a and b) or uncompleted (Fig. 7c) crystallization show additionally that the rupture is initiated at the core of the spherulites (where it is known that stress concentration occurs [29]) and propagates along spherulite radii, inside successive spherulites.

3.2.2. Characterization by small-angle light scattering

SALS patterns of specimens crystallized during cooling in air (Type 3), in iced water (Type 2) and in liquid nitrogen (Type 1) were obtained before and after tensile tests and are displayed in Fig. 8. The undeformed specimens exhibit a four-lobe pattern which is closer to the ideal spherulitic pattern [19, 30] as the degree of crystallinity and the spherulite size increase. So, for specimens quenched in liquid nitrogen (degree of crystallinity 37%), we observed a pattern intermediate between a halo and a four-lobe pattern and the intensity remains strong at the centre of the pattern.

For plastically deformed specimens, it is observed that the lobes are elongated perpendicular to the tensile axis, which can be related to the elongation of the individual spherulites [30], in agreement with the above characterization by optical microscopy. The case of specimen Type 1 (quenched in liquid nitrogen) is more complex since the pattern shows a superimposition of the elongated initial lobes and a system of small additional lobes which can be compared to the ones described by Samuels in other deformed polymers [31], and which were interpreted in terms of the evolution under strain of rod-like arrangements of crystallites. In our case these effects are certainly due to the particular distribution of crystallites in imperfectly developed spherulites.

3.3. Characterization of the phase transformation induced by the plastic deformation

3.3.1. Investigation by differential scanning calorimetry

Small fragments of polybutene (the mass of which was of the order of 1 to 2 mg) were cut out of the rupture region of plastically deformed specimens and analysed with the DSC technique. A plot of the heat-flow rate per unit mass against temperature is presented in Fig. 9a in the case of specimens crystallized in air at 25° C (microstructure Type 3). In Fig. 9a, we compared the melting curves obtained with:

(a) a specimen in Modification II just after

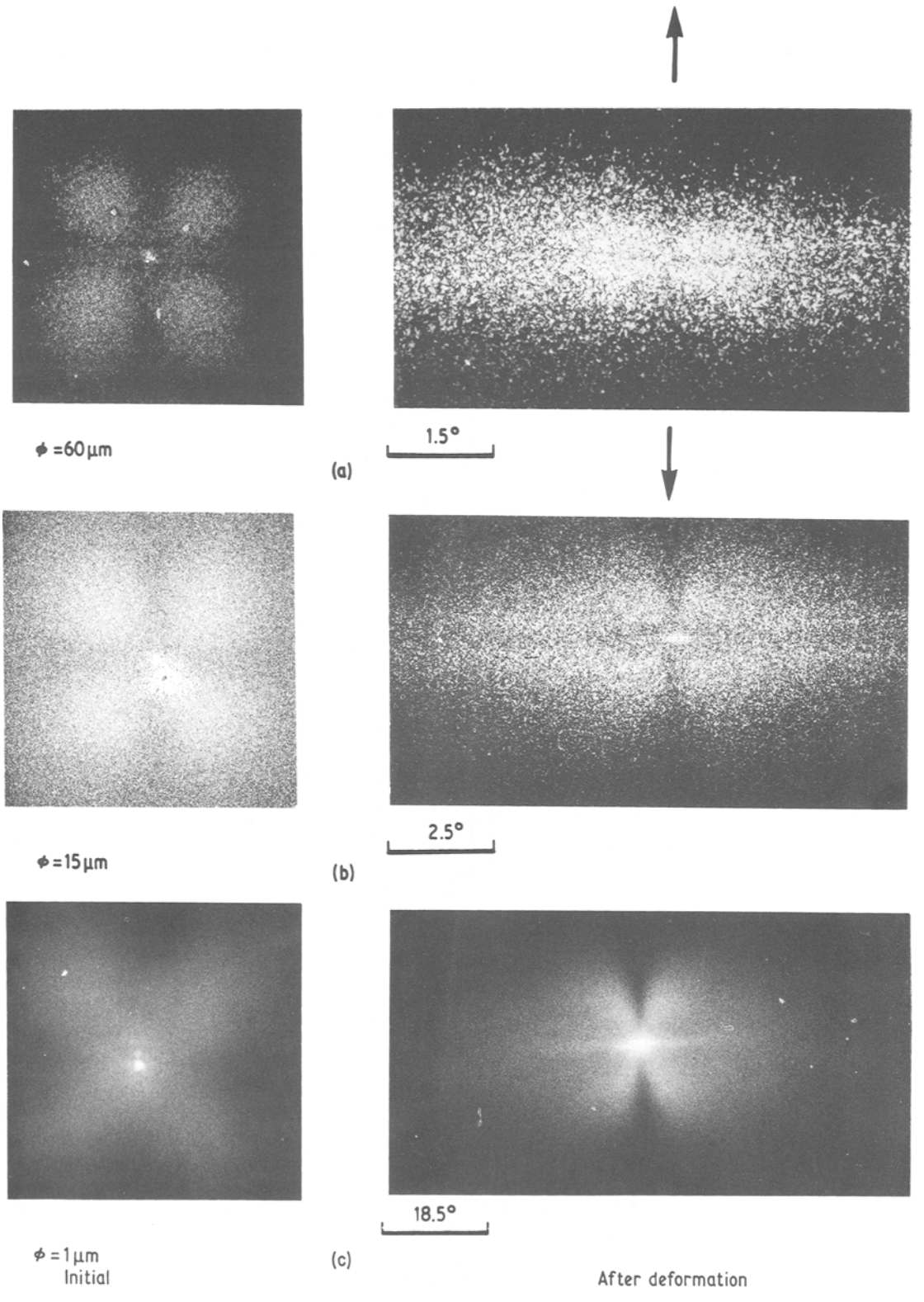

Figure 8 Small-angle light scattering patterns obtained before and after tensile testing of Modification II specimens. (a) Sample crystallized during cooling in air (Type 3); (b) sample crystallized during quenching in iced water (Type 2); (c) sample crystallized during quenching in liquid nitrogen (Type 1).

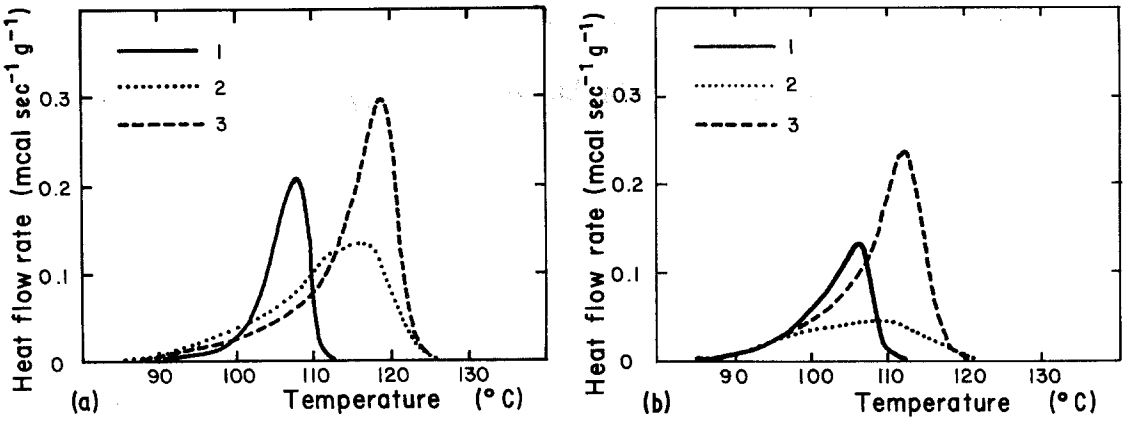

Figure 9 Melting curves of specimens (a) crystallized in air at 25° C (Type 3), (b) crystallized during quenching in liquid nitrogen (Type 1). In this figure we compare the melting curves obtained with: (1) a specimen in Modification II just after crystallization; (2) the same specimen after tensile deformation and rupture; (3) a specimen spontaneously transformed into Modification I.

crystallization;

(b) the same specimen just after tensile deformation and rupture;

(c) a specimen left 15 days at 25° C after its crystallization and so fully transformed into Modification I.

The melting curve of the deformed specimen reaches its maximum at a higher temperature than that of the just-crystallized specimen ($T_m = 116°$ C instead of 108° C). This shift of the melting peak towards higher values after straining a Modification II specimen is of the same order of magnitude as the shift obtained after the ageing of such a specimen and its spontaneous transformation into Modification I ($T_m = 118°$ C). However, the heat of fusion per unit mass for the strained sample is lower than the heat of fusion for the freely transformed one. Eventually, it is observed that the melting curve of the strained sample presents at about 111° C a small shoulder which gives to it a characteristic broad and asymmtric profile.

A similar plot was drawn for samples crystallized during cooling in liquid nitrogen (microstructure Type 1); this is displayed in Fig. 9b. The overall evolution noted above is met again but here the shifts are smaller (from 106 to 109° C after straining and from 106 to 112° C after ageing), and the heat of fusion for the strained specimen is much smaller. Specimens with the three remaining microstructures (Types 2, 4 and 5) were also tested with DSC. The results are in agreement with the ones give above: as the size of the spherulites and the initial crystallinity in Modification II increase, the shift of the melting peak increases, as does the heat of fusion.

Results concerning the evolution of the heat of fusion for the five types of microstructure are reported in Table II. It can be observed that, for each type of microsctructure, the degree of crystallinity in samples initially crystallized in Modification II and transformed into Modification I by stretching is always much lower than in spontaneously transformed ones. On the other hand, the variation of crystallinity resulting from the II → I transformation under strain appears to depend strongly on the initial type of microstructure. This point will be discussed in a further section.

3.3.2. Wide-angle X-ray scattering studies on flat-film photographs

As we found that the DSC peaks of the strained specimens did not correspond any longer to those of the initial Modification II and tended to get closer to those of the Modification I samples, we performed wide-angle X-ray scattering experiments (WAXS) on specimens deformed to rupture in order to check if the initial phase was actually transformed. In the case of microstructure of Type 3 (crystallized in air at 25° C), Fig. 10a and b shows the flat-film diffraction photographs obtained before and after the tensile test. It is obvious from these patterns that the initial system of diffraction rings characteristic of the Modification II (strongest ring indices: 200 and 213 + $\bar{2}$13) is no longer

TABLE II Influence of straining on the crystallinity of polybutene-1 specimens deformed to rupture

Sample	Initial structure	Before straining		After straining	
		ΔH_m (cal g^{-1})	crystallinity (wt %)	ΔH_m (cal g^{-1})	crystallinity (wt %)
1	I	13	43	6.3	21
	II	6.6	36.6	5.7	19.1
2	I	14.1	47	11.9	39.6
	II	6.7	37.5	11.2	37.1
3	I	17.5	58	11.4	38
	II	7.6	42.2	13.6	45.3
4	I	19.2	68	15.7	52.4
	II	8.7	48.6	15.6	52
5	I	22.9	76	19.7	66
	II	9.2	51.1	15.9	53

visible and gives way to a new ring system characteristic of the Modification I (strongest rings: 110, 300 and 220 + 211). It is then ascertained that a plastic deformation transforms the crystallographic lattice of polybutene from the tetragonal phase (Modification II) to the hexagonal phase (Modification I). This transformation was observed in all the specimens tested with different microstructures.

Another piece of information drawn from the WAXS patterns is the deformation texture exhibited by the crystalline fraction after the tensile experiment. It is observed indeed that the diffraction rings present reinforcements of their intensity, which can be interpreted from the orientation of the crystallites, as shown in the diagram of Fig. 10c. This crystalline orientation is observed with all the microstructures but it is more and more pronounced as the size of the spherulites decreases and the corresponding strain at rupture increases. For equivalent spherulite size the orientational ability of the crystallites in Modification II is higher than for Modification I [18].

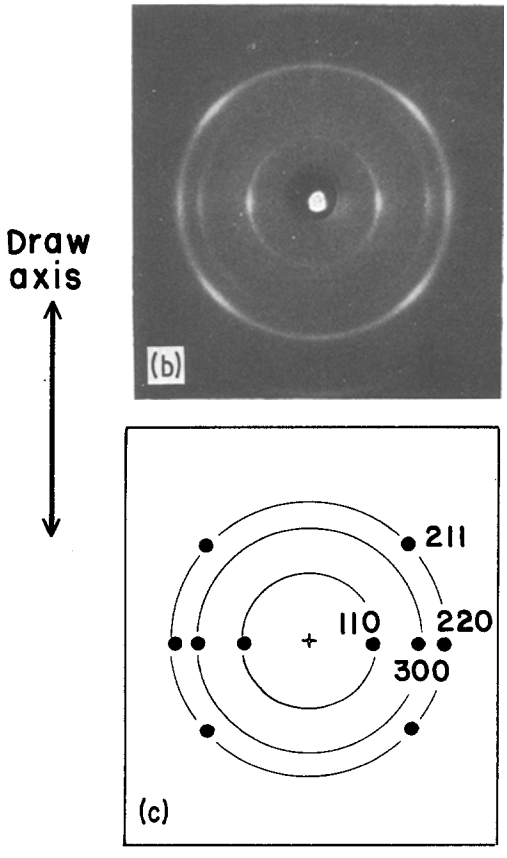

Figure 10 Wide-angle X-ray diffraction patterns of a specimen crystallized in air (Type 3). (a) Before deformation: Modification II reflections; (b) after deformation: Modification I reflections; (c) intensity reinforcements of pattern (b) interpreted from the ideal fibre diffraction pattern of a highly oriented specimen.

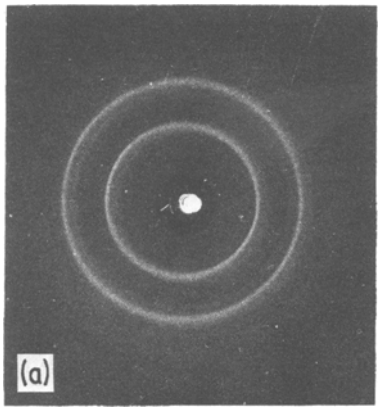

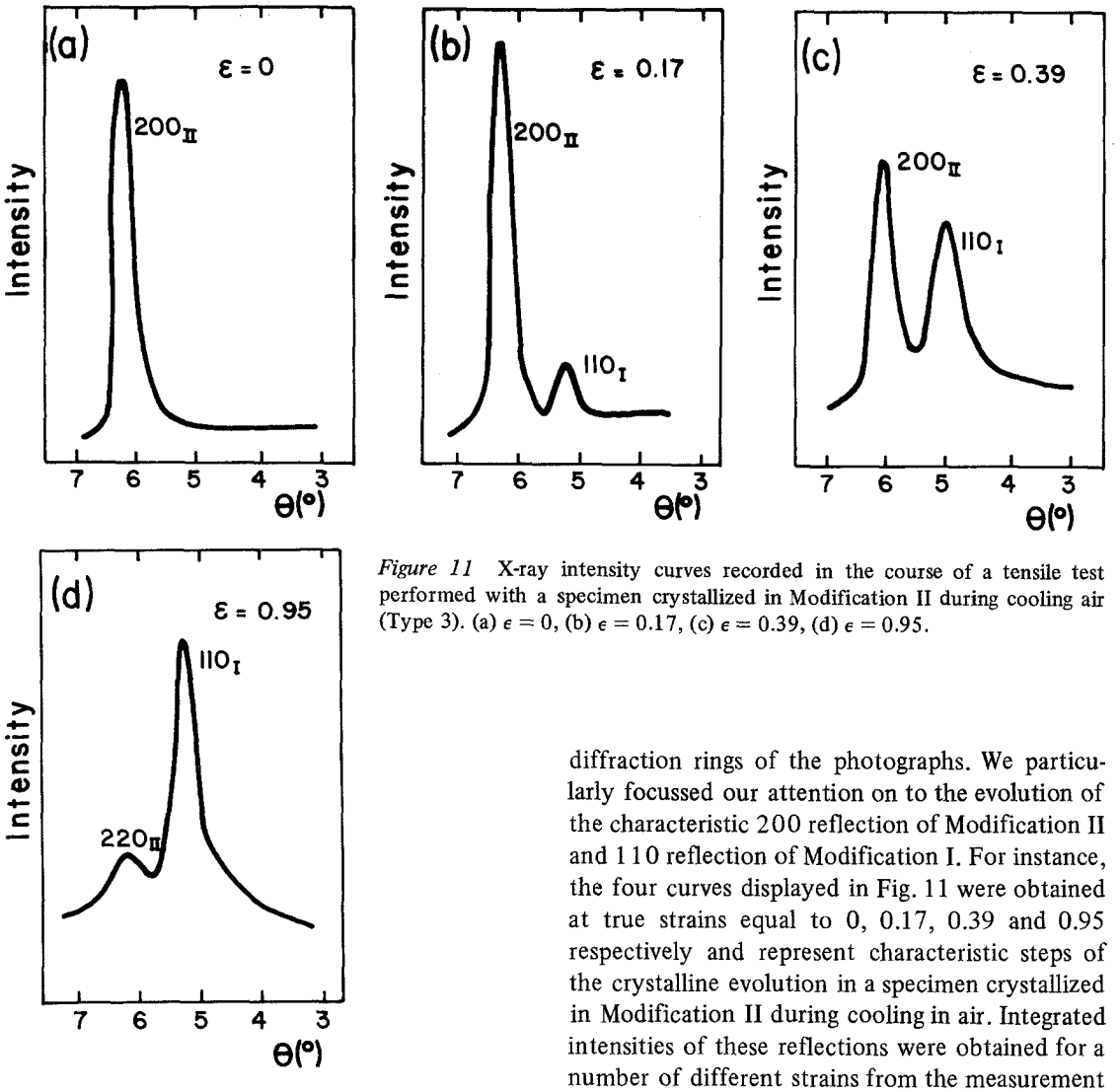

Figure 11 X-ray intensity curves recorded in the course of a tensile test performed with a specimen crystallized in Modification II during cooling air (Type 3). (a) $\epsilon = 0$, (b) $\epsilon = 0.17$, (c) $\epsilon = 0.39$, (d) $\epsilon = 0.95$.

3.3.3. X-ray diffractometry

The above X-ray characterization proved the occurrence of the phase transformation but could not precisely define the evolution of this transformation as a function of the applied tensile strain. Therefore, tensile tests were performed on the goniometer of a diffractometer with the miniaturized tensile machine. The tensile axis was kept vertical and the diffraction plane containing the incident and the investigated diffracted X-ray beams was horizontal. The diffracted intensity was recorded as a function of the diffraction angle, θ, for various stages of deformation.

In comparison to the flat-film diffraction patterns described in the above section, the intensities recorded in these experiments correspond roughly to equatorial scans across the diffraction rings of the photographs. We particularly focussed our attention on to the evolution of the characteristic 200 reflection of Modification II and 1 1 0 reflection of Modification I. For instance, the four curves displayed in Fig. 11 were obtained at true strains equal to 0, 0.17, 0.39 and 0.95 respectively and represent characteristic steps of the crystalline evolution in a specimen crystallized in Modification II during cooling in air. Integrated intensities of these reflections were obtained for a number of different strains from the measurement of the peak areas, and are plotted in Fig. 12.

It can be seen in Fig. 11a, that, due to the early operation of the test just after specimen preparation, the only crystalline phase present at $\epsilon = 0$ is Modification II with its characteristic 200 reflection at $\theta = 6.2°$. The first moment when a noticeable phase transformation could be detected was at $\epsilon = 0.17$ and the corresponding diffraction curve is displayed in Fig. 11b. A new peak appears at $\theta = 5.05°$, which corresponds to the 1 1 0 reflection of Modification I. At the same time, one notes that the initial 200 peak of Modification II does not decrease yet, but rather presents a small enhancement: with the chosen diffraction geometry, this increase in the diffracted intensity can be connected with the orientation of Modification II crystals, the chain axis tending to become parallel to the tensile direction. So, it

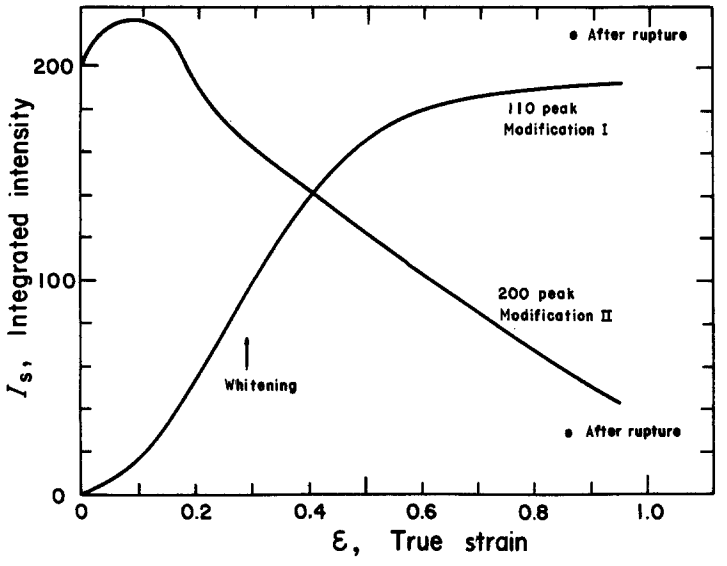

Figure 12 Evolution of the integrated intensitues of the 200 reflection of Modification II and of the 110 reflection of Modification I as a function of the applied true strain.

appears that in the early stages of the deformation, the effect of the crystalline orientation under strain is more important than the reduction of the Modification II percentage due to the II → I phase transformation. The last two steps (Fig. 11c and d) show the gradual increase in the Modification I peak while the Modification II peak decreases to a level near to the lower detection limit of the X-ray counter for a strain equal to 0.95.

The overall evolution of the diffraction peaks can also be followed using the curves of Fig. 12, in which the integrated intensities of the peaks characterizing both phases are plotted as a function of the applied true strain. It is clear that such curves take into account several phenomena: orientation of the initial Modification II, which was discussed above; the II → I phase transformation; and orientation of Modification I crystals, already detected in flat-film diffraction patterns (Fig. 10b). So, because of these texture effects, they cannot be used to calculate the relative amount of each crystal phase. Nevertheless, they provide valuable qualitative information on the evolution of the II → I transformation. For instance, the decrease down to zero of the Modification II peak undoubtly proves the occurrence of the transformation. So, it can be seen that the phase transformation accompanies the plastic deformation up to strains of the order of unity and that Modification I crystals must undergo alone the remaining amount of strain until rupture occurs. The main advantage of our diffractometric procedure is to permit the recording of the diffracted intensity at different steps of the phase transformation in short-duration experiments. The validity of results obtained in longer experiments could be affected by the occurrence of the spontaneous II → I transformation.

Similar investigations were performed on specimens prepared with the other types of microstructure. An identical evolution was recorded in all cases. However, transformation is initiated at a smaller strain as the size of spherulites and the degree of crystallinity increase.

4. Discussion

In the previous section we described experimental results showing that II → I transformation occurred during tensile testing. The evolution of this phase transformation was reported at various stages of the deformation. In this section we discuss the mechanisms which are likely to be involved in the II → I transformation under a tensile stress.

4.1. The II → I transformation at the molecular level

We consider first the modifications induced by the II → I transformation at the molecular level. For this purpose, some crystallographic data concerning both phases are reported in Table III. As already mentioned in Section I, the crystal–crystal transformation involves a change in the chain conformation and requires an elongation of the helical axis from 0.187 to 0.217 nm per chemical repeat unit. So, it can be easily understood that uniaxial drawing in the chain direc-

TABLE III Crystallographic data concerning Modification I and II of isotactic polybutene

Modification	Unit cell	Space group	Unit cell parameters (nm)			Helix conformation	Distance between two monomers (nm)	Crystalline density	Reference
			a	*b*	*c*				
I	Hexagonal (or Rhombohedral)	$R3c$ or $R\bar{3}c$	1.77	1.77	0.65	3_1	0.217	0.95	[1]
II	Tetragonal	$P\bar{4}$	1.485	1.485	2.06	11_3	0.187	0.90	[4]

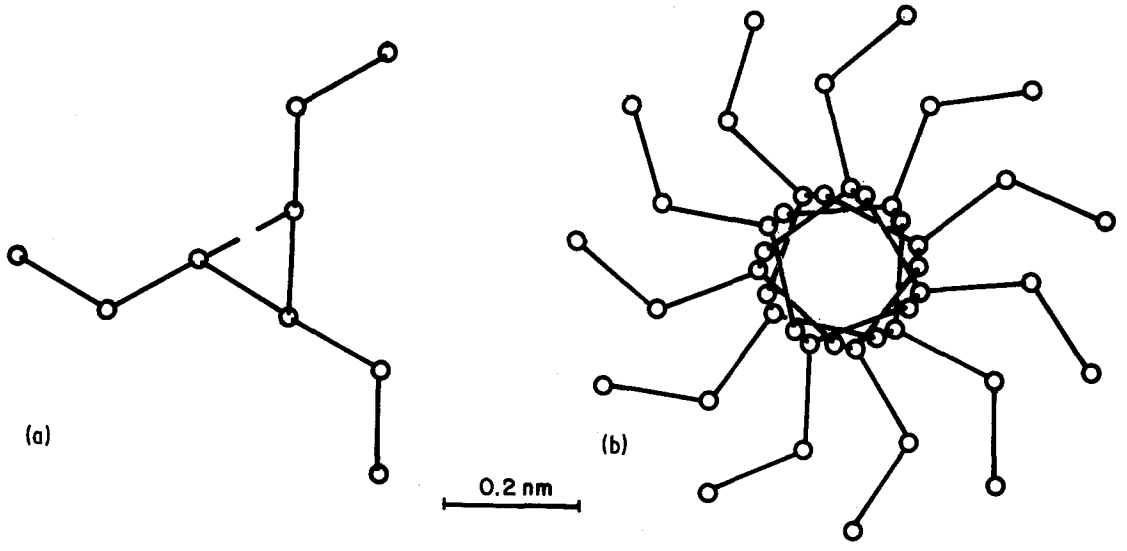

Figure 13 Molecular conformation of isotactic polybutene-1. Projections on the 001 plane of the unit cell. (a) 3_1 helix of Modification I; (b) 11_3 helix of Modification II.

tion will cause axial elongation of the helices, and promote the II → I transformation. At the same time, the chain extension induces a rotation of the lateral groups C_2H_5, as shown in Fig. 13. The cross-sectional area of the helices is reduced and the net result is an increase in crystalline density.

4.2. The II → I transformation within crystallites and spherulites

As shown in Fig. 14, three types of region can be distinguished inside a spherulite, while its response to uniaxial drawing is being investigated:

(a) equatorial regions, where the radial crystallites are nearly perpendicular to the tensile axis;

(b) diagonal regions, where the spherulite radii make an angle lower than 90° with the tensile axis;

(c) polar regions, where the spherulite radii are nearly parallel to the tensile axis.

In these types of region, the deformation mechanisms are different [18, 27, 28] and such differences are expected to have an influence on the II → I transformation.

4.2.1. The II → I transformation for crystallites in equatorial regions

In the equatorial regions, the chain axes are nearly parallel to the drawing direction. Previous experimental observations [16, 18, 27, 28], as well as theoretical calculations [29], have shown that these equatorial regions, and particularly the spherulite core, are subjected to higher strains and stresses. For instance, Wang's calculations [29] have indicated that the strain in the stretching direction is much higher in the equatorial than in the polar regions. As a result, the crystalline lamellae, whose planes are perpendicular to the tensile axis, tend to separate and the molecules

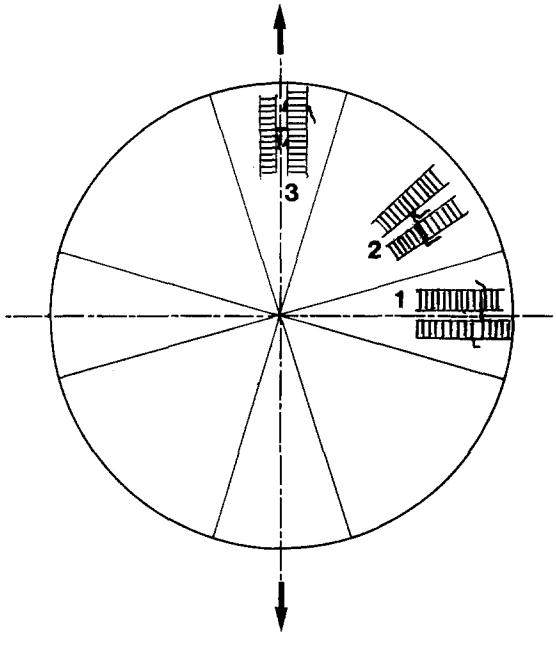

Figure 14 The three types of regions which must be considered inside a spherulite subjected to uniaxial drawing.

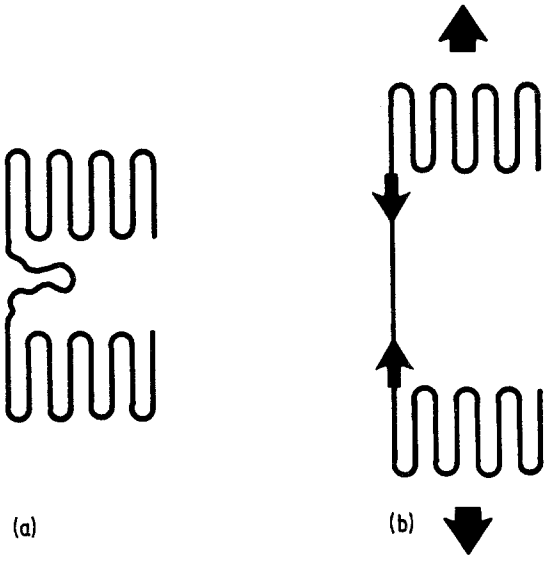

Figure 15 Schematic representation of the part played by extended tie molecules in the initiation of the II → I transformation inside crystalline lamellae.

connecting adjacent crystallites become extended in the amorphous interlamellar layer. These extended tie chains induce tensile stresses on the molecule parts belonging to the crystalline phase. As described in Section 4.1, such tensile stresses in the chain direction will cause axial elongation of the helices and lead to the II → I transformation.

According to the proposed mechanism, the transformation is probably initiated at points where tie molecules re-enter crystalline lamellae (Fig. 15). Then, the elongation of the helical axis and the rotation of the lateral groups can propagate step by step along the molecular chain inside the crystalline lamella. This mode of propagation is to be compared with the propagation of defects, such as Reneker defects involved in annealing mechanisms [32].

4.2.2. The II → I transformation for crystallites in diagonal regions

In the diagonal regions, the crystalline lamellae are not only subjected to a normal strain, which tends to separate them, but also to shear strains [29]. These strains induce a rotation of the lamellae towards the stretching direction, so that, in *in situ* observations, the initial circular shape is converted into an ellipsoidal shape. Concurrently, in each lamella, chain tilt and slip occur under shearing. The main effect of such a deformation is to align the chains more nearly parallel to the tensile axis. So, in diagonal regions, the first stage of the deformation for crystallites initially crystallized in Modification II will consist in an orientation of Modification II chains in the stretching direction. On further stretching, tie molecules are more and more extended, and after orientation of molecular chains in the crystallites, they can apply tensile stresses in the chain direction on molecule parts belonging to the crystalline phase. In the same way as in the equatorial regions, these stresses are likely to induce the phase transformation.

4.2.3. The II → I transformation for crystallites in polar regions

In the polar regions, the chain axis is always approximately perpendicular to the tensile axis. In these regions it seems difficult to initiate the transformation by drawing in the chain direction. Therefore, it is to be expected that deformation will first concern Modification II crystals. For such crystals, the use of a resolved shear strain criterion shows that chain-axis slip is not a favourable deformation mode because of the orientation of the chains perpendicular to the tensile axis. So other deformation modes are likely to be active, for instance twinning, which is often involved in the deformation of polyethylene [28, 34–36], but we have no experimental evidence of such a mechanism in polybutene. In his general model, Peterlin [37–39] assumes that in the polar regions the lateral compression tends to tilt the chains and compress the amorphous layers. The tilt favours chain slip and subsequent break-up of lamellae into smaller folded-chain blocks, separated by cracks. The cracks are bridged by many microfibrils pulled out of the lamellae. In all the supposed mechanisms, chains which were tangential tend to align preferentially in the radial direction. When they have reached a suitable orientation with respect to the tensile axis, the elongation of the helices becomes possible and the phase transformation can occur.

4.2.4. Propagation of the II → I transformation within a spherulite

According to the mechanisms proposed above, the II → I transformation induced by uniaxial drawing will begin in the equatorial regions where, on the one hand, crystallites are subjected to higher strains and stresses, and, on the other hand, molecular chains are almost parallel to the tensile axis. In the other regions, chains have first to reach

an appropriate orientation with respect to the tensile axis before the crystal–crystal transformation can start. In these regions the first detected effect of the plastic deformation must be an orientation of Modification II crystals. As a consequence, the II → I transformation will propagate inside a spherulite from the equatorial to the diagonal and polar regions.

The proposed mechanisms have not been established unquestionably but they do explain the observed deformation morphology and are broadly consistent with the experimental results, particularly the appearance of a dark band characteristic of the presence of Modification I crystals and its propagation from the equatorial towards the diagonal regions.

4.3. Evolution of crystallinity during uniaxial drawing of Modification II specimens

In the models of deformation described in Section 4.2 an important role is played by extended tie molecules. In fact, these extended molecules can act in two opposite ways:

(a) They can pull blocks of crystals out of the crystalline lamellae. This mechanism, generally admitted for the plastic deformation of semicrystalline polymers [40], is accompanied by a lowering of the degree of crystallinity, whatever the initial phase may be. For instance, it can be seen in Table II that, for all types of microstructure, drawing of Modification I samples induces a decrease in the crystalline weight fraction.

(b) They can initiate the II → I transformation in the crystalline lamellae. When the transformation has begun in a lamella, the proposed propagation mode makes it possible to incorporate in the transformed crystallite defects such as loops or chain ends, which were initially rejected at the lamella surface. Such an incorporation corresponds to an increase in crystallinity.

When the phase transformation is induced by plastic deformation, the measured degree of crystallinity is the result of the competition between these two opposite effects. For this reason, it has been noted in Section 3.3 that, for each type of microstructure, the crystallinity level reached in a sample transformed into Modification I by stretching is always much lower than that of a spontaneously transformed specimen.

When we compare the initial crystallinity of a Modification II sample with the crystallinity of the same sample after straining and transformation into Modification I, it can be seen from Table II that the influence of plastic deformation upon crystallinity depends on the initial type of microstructure. In samples of Type 1 (quenching in liquid nitrogen), spherulites are smaller and less crystalline whereas crystallites are thinner, more twisted and less perfect. Many defects, and particularly loops of greater length (Fig. 16a), are rejected at the surface of the imperfect crystals. The incorporation of these defects during the propagation of the II → I transformation is expected to be more difficult because of numerous entanglements in the thicker amorphous layer. These entanglements result from the freezing during quenching of the entangled structure of the melt. On the other hand, as indicated by a greater ductility, the deformation mechanism of these quenched specimens rapidly involves some irreversible chain slip and the destruction of crystalline lamellae by plastic deformation is probably important. The net result is a marked decrease of the degree of crystallinity (about 18 %).

In specimens with coarser and more crystalline spherulites (microstructure Types 3 to 5), the crystallites are thicker, more perfect, with a low

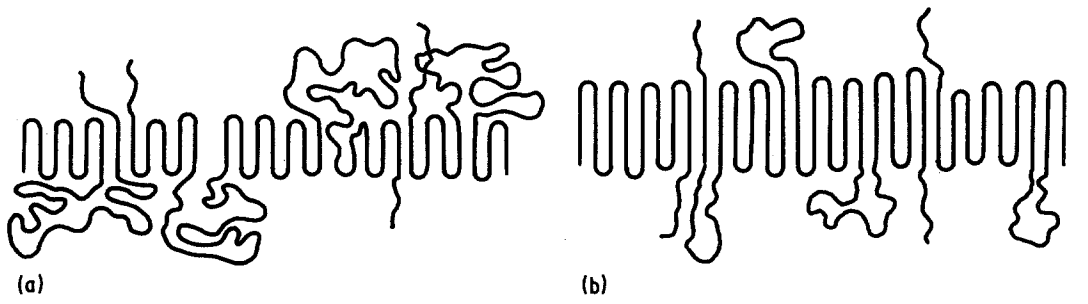

Figure 16 Models of the crystal–amorphous interface. (a) Sample crystallized during quenching in liquid nitrogen (Type 1); (b) samples crystallized at higher temperatures.

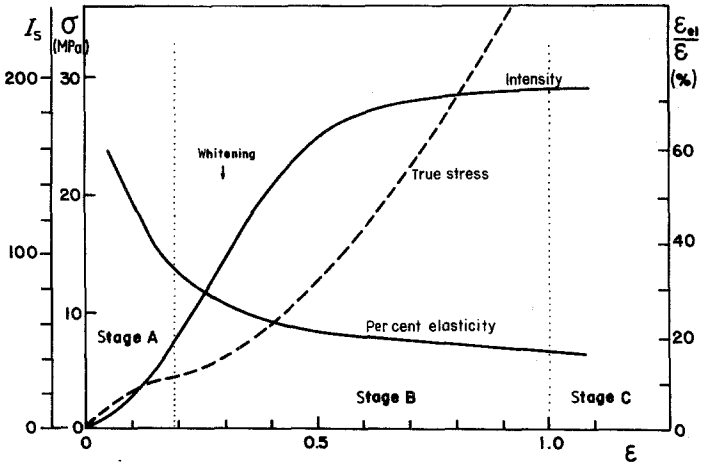

Figure 17 The three stages in the stress–strain behaviour of specimens initially crystallized in Modification II. The experimental data concern specimens crystallized in air (microstructure Type 3).

degree of lamellar twisting. They offer a greater resistance to plastic deformation. As crystal perfection is higher, loops are probably of smaller length (Fig. 16b) and they can more easily be included in transformed cyrstals. The net result is a slight increase in the degree of crystallinity (a few per cent). The case of microstructure Type 2 is intermediate: there is practically no evolution of the degree of crystallinity.

4.4. The three stages in the stress–strain behaviour of Modification II specimens

From the analysis of our experimental results obtained with various techniques (tensile tests, optical microscopy, X-ray diffraction . . .), it follows that three different stages can be distinguished when a polybutene-1 specimen initially crystallized in Modification II is uniaxially drawn. An analogous inference has been drawn by Asada *et al.* [41] from results obtained with other techniques (e.g. infra-red absorption). In order to define more accurately these three characteristic stages, we will mainly use in this section results concerning samples crystallized in air at 25° C (Type 3): some of them are displayed in Fig. 17, in which the strain range corresponding to each stage is indicated. We will also try now to interpret the phenomena observed at each stage by means of the models described in the preceding sections.

4.4.1. Stage A: $0 \leqslant \epsilon \leqslant 0.19$ (for Type 3)

This stage corresponds to the viscoelastic range and to the beginning of the plastic range. In this strain range, the elastic strain ϵ_{el} represents an important part of the total true strain ϵ ($\epsilon_{el}/\epsilon >$ 35%). It is due to the reversible extension of molecules in the amorphous phase and particularly of tie molecules. As mentioned above this extension occurs first in the equatorial regions of the spherulites. The importance of the elastic component decreases when the II → I transformation starts in the equatorial regions, as indicated by the appearance of the 110 reflection of Modification I, which is unambiguously detected about the end of Stage A.

However, the most important feature in this first stage is the orientation of Modification II crystals. It is revealed by an increase in the intensity of the 200 peak of Modification II, at the beginning of the deformation. As discussed in Section 4.2 this orientation concerns crystallites in the diagonal regions of the spherulites.

4.4.2. Stage B: $0.19 \leqslant \epsilon \leqslant 1$ (for Type 3)

The X-ray experiments (Figs 11, 12 and 17) show that the main phenomenon occurring during Stage B is the II → I transformation. According to the model proposed in Section 4.2, the transformation propagates inside the spherulites from the equatorial to the diagonal and polar regions. After transformation into Modification I, the deformation of crystals proceeds according to the deformation mechanisms of Modification I [18]. For instance, a characteristic whitening of the specimen is detected by visual observation for $\epsilon = 0.29$ in the case of microstructure Type 3. Similarly, in the course of *in situ* observations of individual spherulites, a dark band is observed in the equatorial region using optical microscopy. It gradually spreads over almost the whole surface of the spherulite. These observations have been interpreted in a previous paper [18] in terms of

separation and bending of Modification I crystalline lamellae. They also show that the deformation of Modification I crystals, which follows the phase transformation, propagates also from the equatorial towards the diagonal and polar regions. From a mechanical point of view, Stage B is characterized by an important increase in the consolidation rate of the material.

4.4.3. Stage C: $\epsilon \geqslant 1$ (for Type 3)

In this last stage, the transformation into Modification I is complete and Modification I crystals have to undergo alone the remaining amounts of strain up to rupture. As the deformation ability of crystallites in Modification I is lower than in Modification II, intraspherulitic rupture occurs early, especially in specimens with large spherulites [18].

It must be noted that in specimens transformed into Modification I by plastic deformation, the "hard elastic" characteristics of Modification I are far less pronounced: in Stages B and C the elastic component represents only 20% of the total strain in the case of samples of Type 3. The explanation may be the following: in the previous paper [18] an important elastic recovery was observed for Modification I specimens obtained by spontaneous phase transformation after crystallization from the melt. In the present work, Modification I crystals originate from Modification II crystals, which have been orientated and partly destroyed by plastic deformation prior to crystal–crystal transformation. Consequently these Modification I crystalline lamellae are less perfect and specimens exhibit to a lesser degree the characteristics of a "hard elastic" material.

5. Summary and conclusions

Tensile specimens of polybutene-1 initially crystallized in Modification II were tested with a variety of spherulitic morphologies (degree of crystallinity, spherulite size, lamella thickness, etc.). These specimens were found to exhibit a much more pronounced plastic behaviour than specimens fully transformed into Modification I prior to deformation.

It was then observed by different experimental techniques that the most important phenomenon occurring in the course of a tensile test is the II → I phase transformation which takes place in the crystalline lamellae and is induced by plastic deformation. A mechanism has been proposed for this crystal–crystal transformation, in which extended tie molecules in the amorphous phase play an important role in the initiation of the transformation inside crystallites. It was also shown that molecular chains in Modification II crystals have first to be aligned by plastic deformation more nearly parallel to the tensile axis before the phase transformation can start. As a consequence, the II → I transformation propagates inside the spherulites from the equatorial regions perpendicular to the tensile axis towards the diagonal and polar regions.

Finally, it was noted that the quantitative evolution of the transformation as a function of the applied tensile strain and the microstructure of strained specimens were highly dependent of the initial type of spherulitic morphology.

References

1. G. NATTA, P. CORRADINI and I. W. BASSI, *Nuovo Cim. Suppl.*, **15** (1960) 52.
2. J. BOOR Jr and E. A. YOUNGMAN, *J. Polymer Sci.* B **2** (1964) 903.
3. C. D. ARMENIADES and E. BAER, *J. Macromol. Sci. (Phys.)* **B1(2)** (1967) 309.
4. A. TURNER JONES, *J. Polymer Sci.* B **1** (1963) 455.
5. V. PETRACCONE, B. PIROZZI, A. FRASCI and P. CORRADINI, *Europ. Polymer J.* **12** (1976) 323.
6. V. F. HOLLAND and R. L. MILLER, *J. Appl. Phys.* **35** (1964) 3241.
7. G. COJAZZI, V. MALTA, G. CELOTTI and R. ZANNETTI, *Makromol. Chem.* **177** (1976) 915.
8. R. ZANNETTI, P. MANARESI and G. C. BUZZONI, *Chim. Ind. (Milan)* **43** (1961) 735.
9. J. BOOR Jr and J. C. MITCHELL, *J. Polymer Sci.* A **1** (1963) 59.
10. B. H. CLAMPITT and R. H. HUGHES, *ibid.* C **6** (1964) 43.
11. J. P. LUONGO and R. SALOVEY, *ibid.* A-2 **4** (1966) 997.
12. S. Y. CHOI, J. P. RAKUS and J. L. O'TOOLE, *Polym. Eng. Sci.* **6** (1966) 349.
13. R. J. SCHAFFHAUSER, *J. Polymer Sci.* B **5** (1967) 839.
14. A. TURNER JONES, *Polymer* **7** (1966) 23.
15. J. BOOR Jr and J. C. MITCHELL, *J. Polymer Sci.* **62** (1962) 570.
16. R. YANG and R. S. STEIN, *ibid.* A-2 **5** (1967) 939.
17. French Patent No. 2102071 (1971).
18. E. WEYNANT, J. M. HAUDIN and C. G'SELL, *J. Mater. Sci.* **15** (1980) 2677.
19. R. S. STEIN and M. B. RHODES, *J. Appl. Phys.* **31** (1960) 1873.
20. K. SASAGURI, M. B. RHODES and R. S. STEIN, *J. Polymer Sci.* B **1** (1963) 571.
21. J. POWERS, J. D. HOFFMAN, J. J. WEEKS and F. A. QUINN Jr, *J. Res. Nat. Bur. Std* **69A** (1965)

335.
22. I. L. HAY and A. KELLER, *J. Mater. Sci.* 1 (1966) 41.
23. *Idem, ibid* 2 (1967) 538.
24. V. A. KARGIN, G. P. ANDRIANOVA and G. G. KARSASH, *Polymer Sci. USSR* 9 (1967) 289.
25. A. SIEGMAN and P. H. GEIL, in "Plastic Deformation of Polymers" edited by A. Peterlin (Marcel Dekker, New York, 1971) p. 97.
26. E. WEYNANT and J. M. HAUDIN, *Matériaux et Techniques* (March 1981) 57.
27. I. L. HAY and A. KELLER, *Kolloid-Z,* **204** (1965) 43.
28. P. ALLAN and M. BEVIS, *Phil. Mag.* **41** (1980) 555.
29. T. T. WANG, *J. Polymer Sci., Polymer Phys. Ed.* **12** (1974) 145.
30. R. J. SAMUELS, *J. Polymer Sci.* C **13** (1966) 37.
31. *Idem, ibid.* A-2 7 (1969) 1197.
32. D. H. RENEKER, *ibid.* **59** (1962) 539.
33. P. INGRAM, H. KIHO and A. PETERLIN, *ibid.* C **16** (1967) 1857.
34. D. LEWIS, E. J. WHEELER, W. F. MADDAMS and J. E. PREEDY, *J. Appl. Crystallogr.* **4** (1971) 55.
35. *Idem, J. Polymer Sci.* A-2 **10** (1972) 369.
36. J. E. PREEDY and E. J. WHEELER, *J. Mater. Sci.* **12** (1977) 810.
37. A. PETERLIN, *Kolloid Z. Z. Polymere* **233** (1969) 857.
38. *Idem, J. Mater. Sci.* **6** (1971) 490.
39. *Idem, Polymer Eng. Sci.* **17** (1977) 183.
40. J. M. SCHULTZ, "Polymer Materials Science", (Prentice-Hall, Englewood Cliffs, New-Jersey, 1974) p. 499.
41. T. ASADA, J. SASADA and S. ONOGI, *Polymer J.* **3** (1972) 350.

Received 27 April
and accepted 9 September 1981